A molecular dynamics 'Maxwell Demon' experiment for granular mixtures

ALAIN BARRAT and EMMANUEL TRIZAC*

Laboratoire de Physique Théorique (UMR 8627 du CNRS), Bâtiment 210, Université de Paris-Sud, 91405 Orsay Cedex, France

We report a series of molecular dynamics simulations and investigate the possibility to separate a granular mixture of inelastic hard spheres by vigorously shaking it in a box made of two connected compartments. As its one-component counterpart, the system exhibits a 'left–right' symmetry breaking entirely due to the inelasticity of grain–grain collisions, and triggered by increasing the number of particles. In the compartment where the density of grains is larger, we observe a partial segregation with a predominance of heavy particles. However, this compartment still has a higher density of light particles than the other one, which is light-rich. The density, granular temperature and anisotropic pressure profiles are monitored. We also discuss how to construct a relevant order parameter for this transition and show that the resulting bifurcation diagram is dominated by large fluctuations.

1. Introduction

Although granular matter may exhibit similarities with molecular fluids (such as pattern formation), it is nevertheless intrinsically out of equilibrium: The interparticle collisions dissipate kinetic energy and a steady state may only be achieved by a suitable energy supply. As a result, such systems may display many phenomena that are 'forbidden' by the laws of equilibrium statistical mechanics. In the realm of granular gases (dilute systems of macroscopic grains in rapid motion and colliding inelastically), the tendency to form clusters [1–4], non-Gaussian velocity distributions [5–13], long range velocity correlations [12, 14–17] and breakdown of kinetic energy equipartition in a mixture of dissimilar grains [13, 18–21] have been reported.

Another interesting feature, at complete variance with equilibrium phenomenology has been obtained with a simple experiment [22–25]: a vibrated system of grains confined in a box with two connected identical compartments may exhibit a stationary state with spontaneous symmetry breaking (non-equipartition of grains between the two compartments). This clustering phenomenon may be interpreted as a separation in a 'hot' and a 'cold' region, whilst considering that the granular temperature is a direct measure of the mean squared velocity of the particles. In the limit where the exchange of particles between the two compartments

may be considered as an effusion process, Eggers [26] has put forward an analytical approach to explain this apparent intrusion of a 'Maxwell Demon'. On the other hand, Brey *et al.* [27] reported a hydrodynamic mechanism for the symmetry breaking, which becomes operational under some simplifying assumptions in the opposite limit where the size of opening connecting the two compartments is larger than the mean free path of the gas in its vicinity.

In this contribution, we revisit numerically the Maxwell Demon experiment in the latter case, and consider the specific situation of a binary low-density granular mixture, with the aim of investigating whether such a set-up is able to achieve an efficient segregation of the mixture. The model is defined in §2. Making use of molecular dynamics simulations, we discuss in §3 how to construct a relevant order parameter for the transition under study, and show that it is dominated by large fluctuations (as also observed recently in a related context [28]). The two components of the mixture are found to behave differently: heavy particles display a stronger (left–right) asymmetry than the light ones, leading to a separation between a dense gas rich in heavy particles and a dilute light-rich gas. The behaviour of partial densities and granular temperatures are investigated (§4) from which we deduce the different components of the pressure tensor making use of the general equation of state derived in [13]; although the hypothesis of an isotropic pressure given by the ideal gas equation of state is clearly not verified, we show that the no-convection hydrodynamic condition of a divergence-

*Author for correspondence. e-mail: emmanuel.trizac@th.u-psud.fr

free pressure tensor ($\nabla \cdot P = 0$) is obeyed, taking into account anisotropies, boundaries and corrections to the ideal gas equation of state. Conclusions are finally drawn in §5.

2. The model

The system is made of N inelastic hard discs evolving in a $S \times L$ two-dimensional box, losing energy at inter-particle collisions and gaining energy through collisions with two vibrating walls situated at $y = 0$ and $y = L$ (figure 1). The particles have diameters σ_i and masses m_i, $i = 1, 2$. A binary collision between grains of species i and j is momentum conserving and dissipates kinetic energy: the collision i–j is characterized by the coefficient of normal restitution α_{ij}. Accordingly, the pre-collisional velocities $(\mathbf{v}_i, \mathbf{v}_j)$ are transformed into the post-collisional couple $(\mathbf{v}'_i, \mathbf{v}'_j)$ such that

$$\mathbf{v}'_i = \mathbf{v}_i - \frac{m_j}{m_i + m_j}(1 + \alpha_{ij})(\widehat{\boldsymbol{\sigma}} \cdot \mathbf{v}_{ij})\widehat{\boldsymbol{\sigma}}, \tag{1}$$

$$\mathbf{v}'_j = \mathbf{v}_j + \frac{m_i}{m_i + m_j}(1 + \alpha_{ij})(\widehat{\boldsymbol{\sigma}} \cdot \mathbf{v}_{ij})\widehat{\boldsymbol{\sigma}}, \tag{2}$$

where $\mathbf{v}_{ij} = \mathbf{v}_i - \mathbf{v}_j$ and $\widehat{\boldsymbol{\sigma}}$ is the centre-to-centre unit vector from particle i to j. Note that $\alpha_{ij} = \alpha_{ji}$ to ensure the conservation of total linear momentum $m_i\mathbf{v}_i + m_j\mathbf{v}_j$. The total density is denoted ρ, and the partial densities $\rho_i = x_i\rho$ (the number fractions x_i are such that $\sum_i x_i = 1$). The granular temperature of species i is T_i, defined from the mean kinetic energy of subpopulation i, by analogy with the usual temperature of elastic gases: $T_i = \langle m_i v_i^2 \rangle / d$, where d is the space dimension (here $d = 2$). In the remainder of the paper this granular temperature will be coined 'temperature' for simplicity.
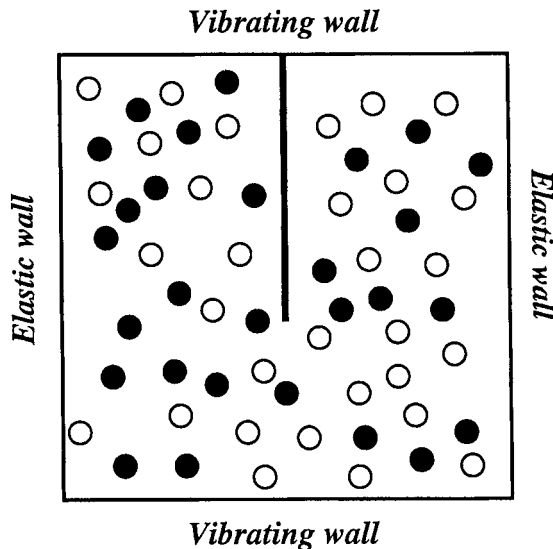
The box is divided into two compartments of width $S/2$ by a wall parallel to Oy starting at height y_0. The walls located at $x = 0$ and $x = S$ are elastic, while those at $y = 0$ and $y = L$ are vibrating and thus inject energy into the system. For simplicity, the two vibrating walls are taken to move in a saw-tooth manner, so that a colliding particle at $y = 0$ (resp. $y = L$) always finds the wall to move 'upwards' (resp. 'downwards') with the same velocity v_0 (resp. $-v_0$). In addition, the amplitude of the vibration is considered to vanish (i.e. to be much smaller than the local mean free path [26, 27]), so that the walls are located at the fixed positions $y = 0$ and $y = L$: the y-component velocity of a particle colliding with the wall at $y = 0$ (resp. $y = L$) is therefore changed according to $v'_y = 2v_0 - v_y$ (resp. $v'_y = -2v_0 - v_y$). Since we consider vigorous shakings, the gravitational field has not been included in the analysis.

For simplicity, we have considered equimolar mixtures ($N_1 = N_2$) of particles having the same diameter ($\sigma_1 = \sigma_2$) but different masses. Various mass ratios $m_1/m_2 \in [1:5]$ have been studied,† so that the species 1 is always the heavier particle. We have run molecular dynamics simulations [29] changing N either at constant packing fraction (equal to $\pi\rho\sigma^2/4$ in two dimensions) or at constant σ_i, with the same qualitative observations. The numerical results we will present correspond to a fixed low mean packing fraction $\eta_0 = 0.015$ (the inelastic collapse [3] occurring if the mean density exceeds a low threshold), and to equal coefficients of restitution $\alpha_{ij} = 0.9$, close to experimentally relevant values. We have investigated other values of the restitution coefficients between 0.7 and 0.9, and two different aspect ratios, $L = S$ and $L = 2S$, with the same qualitative results.

3. Bifurcation diagram and large fluctuations

For a one component system, it has been shown from a hydrodynamic approach [27] that, as the number of particles in the box (N) is increased, a transition occurs at a certain threshold N^*: for $N < N^*$, the system is symmetric, i.e. the mean number of particles in each compartment is $N/2$ while, for $N > N^*$, one of the compartments becomes more populated and colder than the other. This hydrodynamic study relies on the assumption of an isotropic pressure given by the ideal gas equation of state [27]. At a given inelasticity (i.e. at

Vibrating wall

Vibrating wall

Figure 1.   Schematic picture of the set-up.

† In the context of homogeneously heated binary granular mixtures, it has been shown in [21] that the influence of size asymmetry on the kinetic energy non-equipartition is much less important than that of mass asymmetry. We therefore restrict our study to the influence of the latter parameter.

given values of the restitution coefficients), the control parameter (governing the transition from the symmetric to the asymmetric situation) is proportional to $N\sigma^{d-1}/S$, where σ is the particle diameter [27]. At fixed reduced density $n = N\sigma^d/(LS)$ the above parameter is proportional to $N^{1/d}$, while at fixed size σ it scales like N.

The 'order parameter' of this transition was defined in [26, 27] as the time average $\langle \epsilon \rangle$ of the asymmetry ϵ:

$$\epsilon = \frac{N - 2N^{\text{left}}}{2N}, \tag{3}$$

where N^{left} is the number of particles in the left compartment. In addition to the global ϵ, we may introduce two relevant asymmetry parameters for each type of particles

$$\epsilon_i = \frac{N_i - 2N_i^{\text{left}}}{2N_i}, \quad i = 1, 2. \tag{4}$$

For a given simulation time, if one computes $\langle \epsilon_i \rangle$ for the binary mixture (or $|\langle \epsilon_i \rangle|$ to have a positive quantity), a left–right symmetry breakdown is shown (see figure 2). The asymmetry is more pronounced for heavy particles ($|\langle \epsilon_1 \rangle| > |\langle \epsilon_2 \rangle|$), and $|\langle \epsilon_1 \rangle|$ increases with the mass ratio m_1/m_2. On the other hand, the light particle asymmetry decreases with m_1/m_2. At this point we conclude that the compartment with larger global density is heavy-rich, while the lighter particles are more uniformly distributed and therefore the less populated compartment is richer in light particles.

However, for symmetry reasons, one should expect that the mean value $\langle \epsilon \rangle$ (and the $\langle \epsilon_i \rangle$) always vanish for sufficiently long simulation times, so that these quantities are arbitrary and do not provide relevant order parameters. Inspection of the time behaviour of N^{left} confirms this picture (see figure 3(*a*)), which is made more quantitative by computing the probability distribution function of ϵ over very long runs and various initial conditions (see figure 3(*b*)). At small N, ϵ fluctuates around 0 and its standard deviation increases with N. As N increases, the asymmetric configurations become stable but the system continuously jumps from one of the possible asymmetric situations to the other, still spending some time in between close to the symmetric state. When N further increases, the residence time spent in each of the asymmetric states increases and may eventually overcome the simulation time: for $N \gg N^*$, starting from a symmetric situation, the system quickly evolves into an asymmetric configuration, in which one compartment is strongly over-populated, and remains in this situation for all the simulation time. For larger simulation times however the symmetry would be restored. The situation is thus analogous to that of a two-state system, in which the energy barrier between two symmetric states increases with system size. This behaviour is reminiscent of that recently reported in [28]: in this study of a translational symmetry breaking as the aspect ratio of the simulation box is changed (without a separating wall), large fluctuations have been shown to occur over a wide region around a hydrodynamically predicted threshold
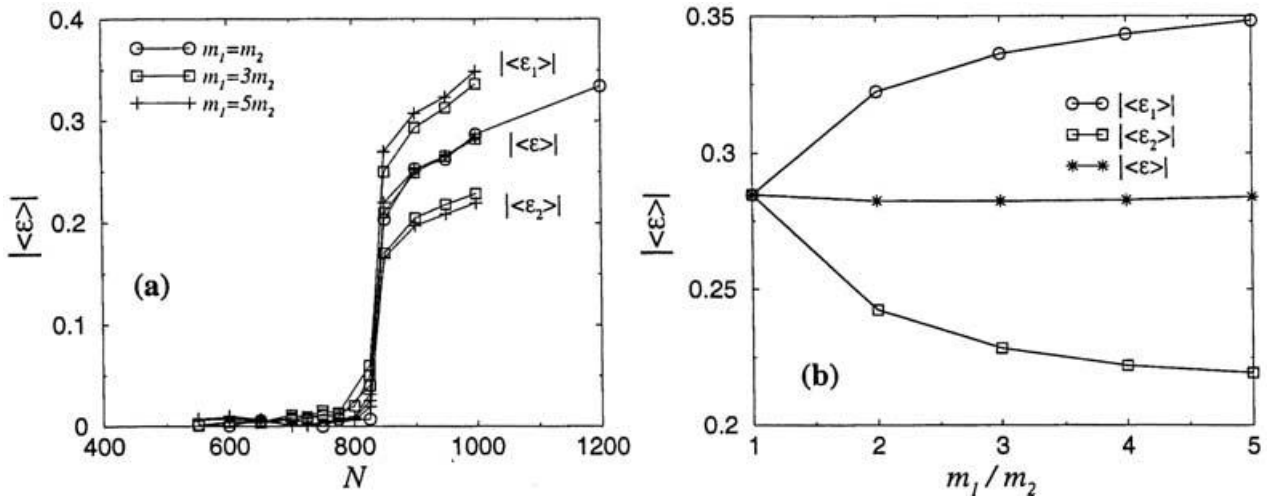

Figure 2. (*a*) Asymmetry parameters $|\langle \epsilon \rangle|$ and $|\langle \epsilon_i \rangle|$ versus number of particles for three different mass ratios and a given simulation time, i.e. number of collisions per particle. Here, all the inelasticity parameters are taken equal: $\alpha_{11} = \alpha_{12} = \alpha_{22} = 0.9$. The opening connecting both compartments is 40% of the total height of the simulation cell ($y_0 = 0.4L$). (*b*) Asymmetry parameters versus mass ratio, at fixed number of particles $N = 1000$ and $\alpha_{ij} = 0.9$. As the mass ratio increases the asymmetry increases for the heavy particles and decreases for the light ones. As emphasized in the text, these figures depend on the simulation time available.
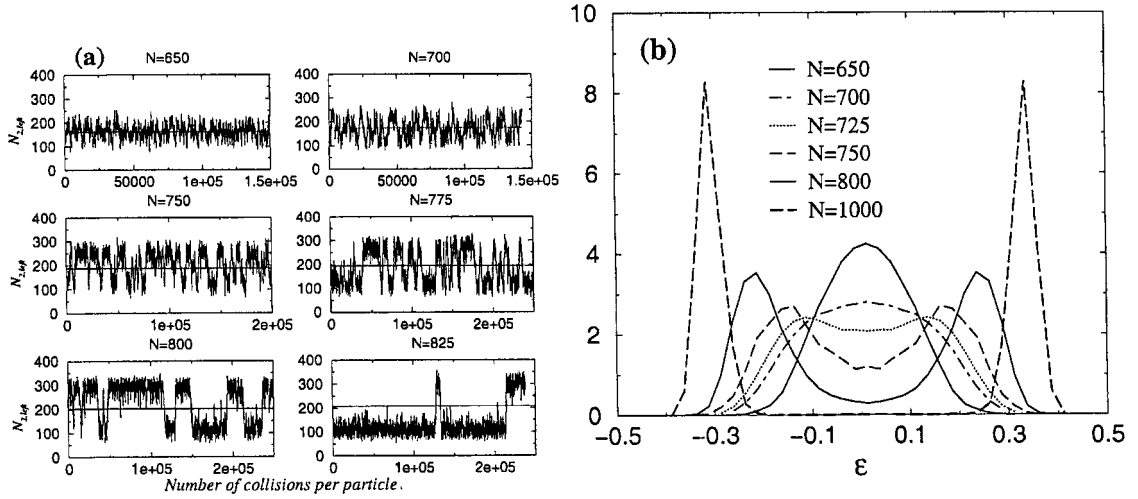
Figure 3. (*a*) Number of particles of type 2 in the left compartment as a function of time (measured in number of collisions per particle), for various values of N, and $m_1/m_2 = 3$. In all cases, the horizontal lines correspond to the symmetric situation $N^{\text{left}} = N^{\text{right}}$. (*b*) Probability distribution function of ϵ for $m_2/m_1 = 3$.
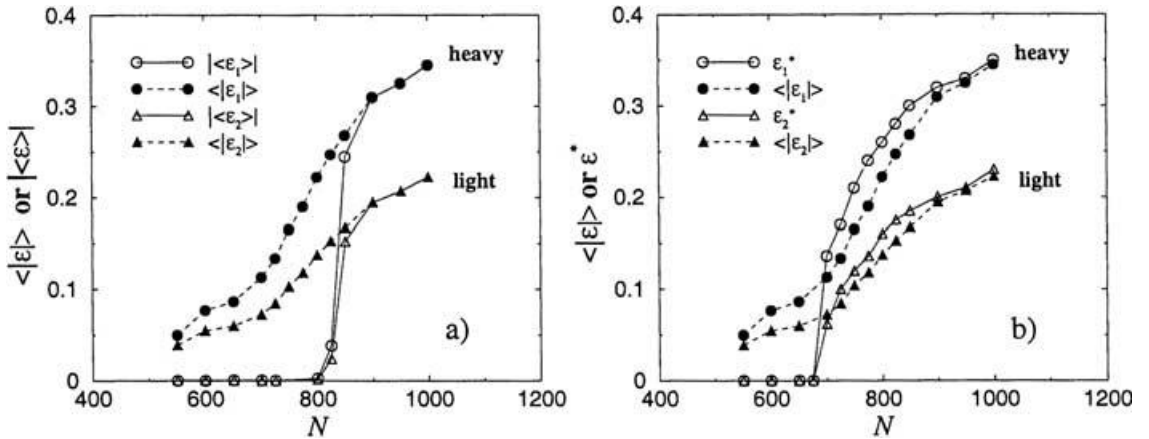

Figure 4. (*a*) Asymmetry parameters $\langle|\epsilon_i|\rangle$ and $|\langle\epsilon_i\rangle|$ versus number of particles for $m_1 = 5m_2$. The inelasticity coefficients are the same as in figure 2 ($\alpha_{ij} = 0.9$). (*b*) Comparison of the most probable values ϵ_i^* with $\langle|\epsilon_i|\rangle$ for the same parameters as in (*a*).

value beyond which the homogeneous system becomes unstable.

In any case, $|\langle\epsilon\rangle|$ vanishes for any N for long enough simulations, and does not provide an acceptable order parameter. There are then *a priori* two possibilities to construct such a quantity: (a) by time averaging $|\epsilon|$ or (b) by extracting the most probable (say positive) value ϵ^* of ϵ from its probability distribution function (pdf, see figure 3), averaged over the simulation time and over various initial conditions. Note that this pdf, and thus both possible definitions, are not sensitive to the length of the simulations (except for very small simulation times).† We compare in figure 4 these two definitions

with the previous one, $|\langle\epsilon\rangle|$, computed again for a given (large) simulation time. Since ϵ fluctuates around 0 even at small N, the $\langle|\epsilon_i|\rangle$ depend rather smoothly on N, and therefore do not allow a clear definition of a critical number of particles. On the other hand, the most probable values ϵ_i^* allow one to define a critical region, being identically 0 at small N and taking positive values above a certain threshold (see figure 4). When N is large enough, the probability distribution functions of the ϵ_i become sharply peaked around the ϵ_i^* so that both quantities ϵ_i^* and $\langle|\epsilon_i|\rangle$ become close; moreover, these pdfs take extremely small values in the vicinity of $\epsilon_i = 0$: this corresponds to the fact that the system is stuck for long times in one of its two most probable states, so that the computation of $|\langle\epsilon_i\rangle|$ coincides with that of $\langle|\epsilon_i|\rangle$, or ϵ_i^*.

† Note that similar definitions could also be used in the context of [28] to construct order parameters.

4. Density profiles and pressure tensor

Instantaneous typical configurations are displayed in figure 5 for various values of N and mass ratio m_1/m_2. From the coarse grained local packing fractions $\eta_i(x, y)$, we define x-averaged quantities in each compartment:

$$\eta_i^l(y) = \frac{2}{S} \int_0^{S/2} dx \eta_i(x, y),$$

$$\eta_i^r(y) = \frac{2}{S} \int_{S/2}^{S} dx \eta_i(x, y), \quad i = 1, 2. \quad (5)$$

These quantities are averaged over time for one run between two successive 'flips' (see § 3), but not averaged over various runs since the asymmetry would then be lost. The corresponding density and temperature profiles are shown in figure 6 for $N = 1000$, well above the bifurcation point. One may observe that in the asymmetric situation, the densities are different even for $y < y_0$, i.e. not only where the compartments are physically separated.

Two-dimensional plots of the coarse grained densities $\eta_i(x, y)$ are displayed in figure 7 for two values of the number of particles, well below and well above the bifurcation. Below the transition, translational invariance in x holds in the whole box, while above, the densities and temperatures are almost independent of x in each compartment, but are discontinuous at $x = S/2$ for $y > y_0$ because of the separating wall; at $y < y_0$ but close to y_0 a quite sharp change is observed in the vicinity of $x = S/2$. At small y the x gradients are smaller.

In the hydrodynamic study of [27], the ideal gas form for the pressure constitutes a fundamental hypothesis which allows for an analytic treatment; moreover, the pressure is assumed to be isotropic. However, anisotropic energy injection mechanisms lead to anisotropic pressure tensors, especially near vibrating walls [13, 30]. Knowing the density and pressure profiles for our system, one may compute the two components P_{xx} and P_{yy} of the pressure tensor from a given equation of state. We consider the generic expression derived in [13] within Enskog–Boltzmann kinetic theory. For a homogeneous and isotropic mixture with partial temperatures T_i, number fractions x_i and without any approximation on the
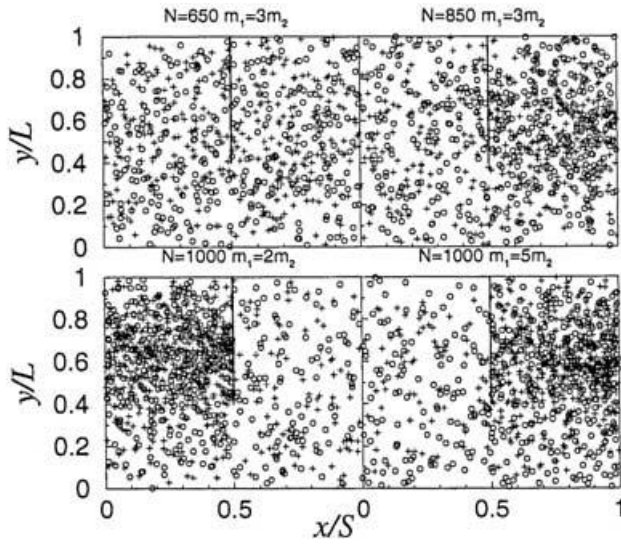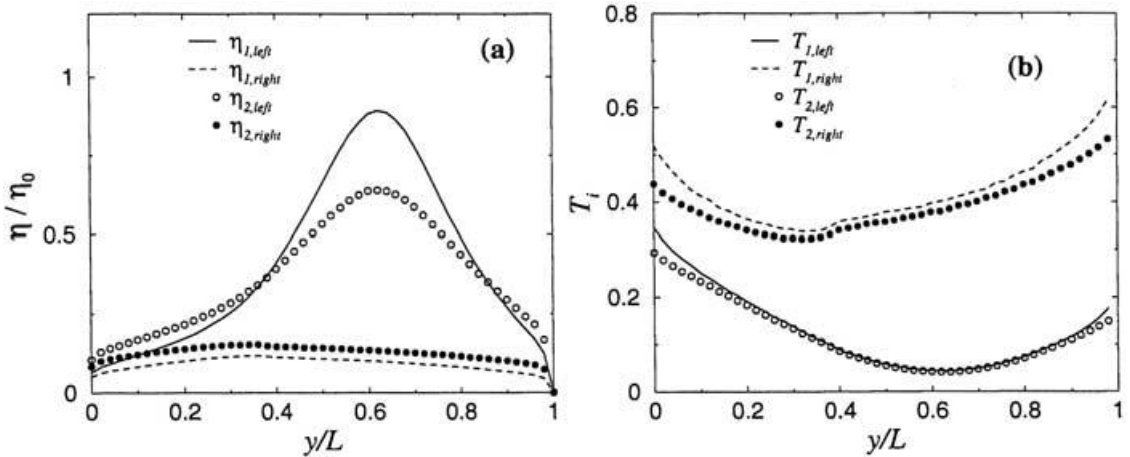

Figure 5. Typical instantaneous snapshots. Heavy particles (label 1) are denoted by a plus, and light particles (label 2) by a circle. Top left: $N = 650$, $m_1 = 3m_2$; top right: $N = 850$, $m_1 = 3m_2$; bottom left $N = 1000$, $m_1 = 2m_2$; bottom right: $N = 1000$, $m_1 = 5m_2$.

Figure 6. (*a*) Density and (*b*) temperature profiles for $N = 1000$, $m_1 = 2m_2$. The left compartment ($0 < x < S/2$) is denser and colder than the right one. In the right compartment, the light particles are denser than the heavy ones. The mean packing fraction, averaged over the whole system is $\eta_0 = 0.015$. The ratio $\eta(y)/\eta_0$ is also the ratio $\rho(y)/\rho$ of local density normalized by the mean one. The separation between the two compartments is located at $x = S/2$; $0.4 < y/L < 1$.
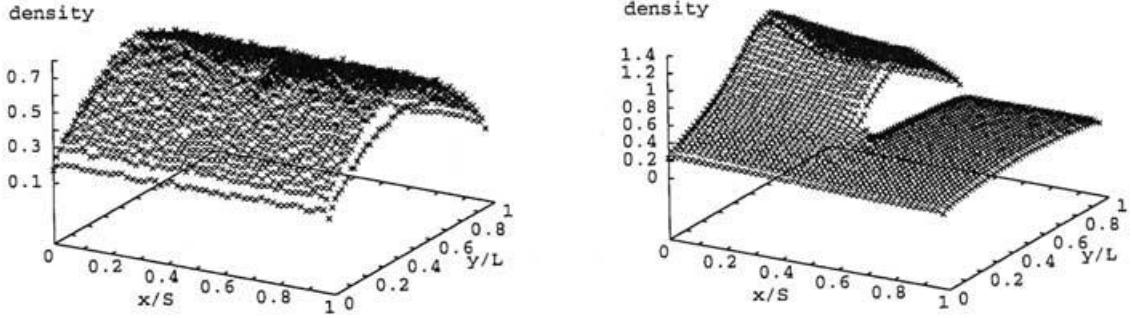
Figure 7.   Averaged local density of the particles of type 2 (light component) for $N = 400$ (left panel) and $N = 900$ (right panel). The separating wall is at $x = S/2$, $y > y_0 = 0.4L$ and $m_1 = 3m_2$ in both cases.
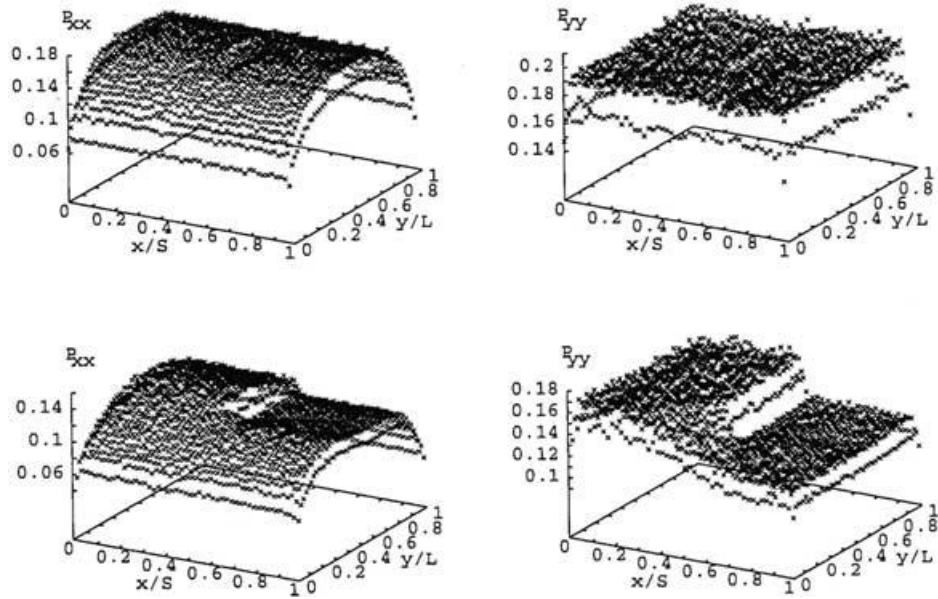

Figure 8.   Components of the pressure tensor P_{xx} (left) and P_{yy} (right), as given by the equation of state (equation (6)), for $N = 600$ (top) and $N = 900$ (bottom). Here, $m_1/m_2 = 3$ and $\alpha_{ij} = 0.9$. For $N = 900$, the right compartment ($x > S/2$) is more populated, colder and at a lower pressure.

single particle velocity distribution, it was obtained that

$$P = \sum_i \rho_i T_i + \rho\eta \, 2^{d-1} \sum_{i,j} x_i x_j \frac{m_j}{m_i + m_j}(1 + \alpha_{ij})T_i \frac{\sigma_{ij}^d}{\langle \sigma^d \rangle}\chi_{ij},$$

(6)

where d denotes the space dimension, $\sigma_{ij} = (\sigma_i + \sigma_j)/2$ and $\langle \sigma^d \rangle = \sum_i x_i \sigma_i^d$. The χ_{ij} are the *a priori* unknown pair distribution functions at contact; these quantities embody the correction to the ideal gas equation of state, and since we are considering a dilute system, it is sufficiently accurate to assume $\chi_{ij} = 1$ (low density limiting value). The values of P_{xx} and P_{yy} are finally obtained by substituting T_i in (6) respectively by T_{ix} and

T_{iy} (i.e. the mean square x or y components of the particle velocities).

The results are summarized in figure 8, where we plot $P_{xx}(x, y)$ and $P_{yy}(x, y)$ for $N = 600$ and $N = 900$. Below the transition ($N = 600$), the picture is similar to the one without a separating wall, and the pressure tensor is x independent. One therefore has $\partial_x P_{xx} = \partial_x P_{yy} = \partial_y P_{yy} = 0$. However, for $N = 900$ (above the transition), the yy components are no longer equal in the left and right sides, while the xx components are equal only for $y < y_0$ where the separation begins. One still observes $\partial_x P_{xx} = \partial_y P_{yy} = 0$ in each compartment, except close to the extremity of the separating wall ($x = S/2$, $y = y_0$), but for $y > y_0$ the separating wall allows for different values of the pressure components. Moreover $\partial_x P_{yy} \neq 0$ for $y < y_0$ while for $y > y_0$, $\partial_x P_{yy} = 0$ in each compartment (except close to $x = S/2$), with a discontinuity at

$x = S/2$. It is worth noting that the denser compartment is also the one where both components of the pressure tensor are lower, since it is much 'colder' than the dilute compartment.

This analysis shows that both above and below the symmetry breaking, the (anisotropic) pressure tensor as computed from equation (6) is divergence free: $\partial_x P_{xx} + \partial_y P_{yy} = 0$. This 'hydrostatic' requirement follows from the condition of a vanishing flow field, and in spite of the low mean densities considered here, would not be fulfilled on restricting P_{xx} and P_{yy} to their ideal parts.

5. Conclusions

For a one component granular gas enclosed in a box made of two connected compartments, a vigorous shaking is known to promote a symmetry breakdown and separate the system into a cold and dense region on the one hand, and a hot and dilute part on the other hand (so called 'Maxwell Demon' experiment). In addition, in a binary granular mixture, heavy and light grains generically have different granular temperatures. In this contribution, we have combined both aspects (Maxwell Demon and mixture) to investigate the possibility to separate the two components of the mixture. Our molecular dynamics results show a spontaneous symmetry breaking as the number of particles is increased, all other parameters being kept constant. The denser compartment then appears to be rich in heavy particles, but this partial segregation is such that this compartment is also richer in light particles than the other half of the confining box (which is however the light-rich one). It therefore seems that such a set-up cannot achieve an efficient segregation (although a possibility would be to isolate the dense compartment and iterate the process with this non-equimolar mixture).

The transition reported here is not *stricto sensu* a phase transition, since the control parameter is the system size. As a consequence, fluctuations can always bring the system from one of the asymmetric states to the other, as e.g. for a finite size Ising model below its critical temperature. We have discussed the consequences of this feature on the definition of a relevant order parameter to characterize the bifurcation.

We finally note that the experimental realization of the two-dimensional situation investigated here seems feasible, for instance by adapting the configuration used in [6] (friction with the walls confining the system in a 2D slab might play a role, and has not been considered here). The experimental signature of the

large fluctuations which invalidate hydrodynamic approaches seems an interesting issue.

References

[1] KADANOFF, L., 1999, *Rev. mod. Phys.*, **71**, 435.
[2] GOLDHIRSCH, I., and ZANETTI, G., 1993, *Phys. Rev. Lett.*, **70**, 1619.
[3] MCNAMARA, S., and YOUNG, W. R., 1994, *Phys. Rev. E*, **50**, R28; 1996, *Phys. Rev. E*, **53**, 5089.
[4] TRIZAC, E., and BARRAT, A., 2000, *Eur. Phys. J. E*, **3**, 291.
[5] LOSERT, W., COOPER, D. G. W., DELOUR, J., KUDROLI, A., and GOLLUB, J. P., 1999, *Chaos*, **9**, 682.
[6] ROUYER, F., and MENON, N., 2000, *Phys. Rev. Lett.*, **85**, 3676.
[7] VAN NOIJE, T. P. C., and ERNST, M. H., 1998, *Granular Matter*, **1**, 57.
[8] PUGLISI, A., LORETO, V., MARCONI, U. M. B., and VULPIANI, A., 1999, *Phys. Rev. E*, **59**, 5582.
[9] NIE, X., BEN-NAIM, E., and CHEN, S. Y., 2000, *Europhys. Lett.*, **51**, 679.
[10] CAFIERO, R., LUDING, S., and HERRMANN, H. J., 2000, *Phys. Rev. Lett.*, **84**, 6014.
[11] BARRAT, A., BIBEN, T., RACZ, Z., TRIZAC, E., and VAN WIJLAND, F., 2002, *J. Phys. A: Math. Gen.*, **35**, 463.
[12] PREVOST, A., EGOLF, D. A., and URBACH, J. S., 2002, *Phys. Rev. Lett.*, **89**, 084301.
[13] BARRAT, A., and TRIZAC, E., 2002, *Phys. Rev. E*, **66**, 051303.
[14] VAN NOIJE, T. P. C., ERNST, M. H., TRIZAC, E., and PAGONABARRAGA, I., 1999, *Phys. Rev. E*, **59**, 4326.
[15] BLAIR, D. L., and KUDROLLI, A., 2001, *Phys. Rev. E*, **64**, 050301(R).
[16] MOON, S. J., SHATTUCK, M. D., and SWIFT, J. B., 2001, *Phys. Rev. E*, **64**, 031303.
[17] PAGONABARRAGA, I., TRIZAC, E., VAN NOIJE, T. P. C., and ERNST, M. H., 2002, *Phys. Rev. E*, **65**, 011303.
[18] GARZÓ, V., and DUFTY, J., 1999, *Phys. Rev. E*, **60**, 5706.
[19] FEITOSA, K., and MENON, N., 2002, *Phys. Rev. Lett.*, **88**, 198301.
[20] WILDMAN, R. D., and PARKER, D. J., 2002, *Phys. Rev. Lett.*, **88**, 064301.
[21] BARRAT, A., and TRIZAC, E., 2002, *Granular Matter*, **4**, 57.
[22] SCHLICHTING, H. J., and NORDMEIER, V., 1996, *Math. Naturwiss. Unterr.*, **49**, 323.
[23] VAN DER WEELE, K., VAN DER MEER, D., VERSLUIS, M., and LOHSE, D., 2001, *Europhys. Lett.*, **53**, 328.
[24] VAN DER MEER, D., VAN DER WEELE, K., and LOHSE, D., 2002, *Phys. Rev. Lett.*, **88**, 174302.
[25] MIKKELSEN, R., VAN DER MEER, D., VAN DER WEELE, K., and LOHSE, D., 2002, e-print: cond-mat:0210128.
[26] EGGERS, J., 1999, *Phys. Rev. Lett.*, **83**, 5322.
[27] BREY, J. J., MORENO, F., GARCIA-ROJO, R., and RUIZ-MONTERO, M. J., 2001, *Phys. Rev. E*, **65**, 011305 (NB: in equation (2), there should be $(d + 2)^3$ instead of $(d + 3)^3$ in the denominator).
[28] MEERSON, B., PÖSCHEL, T., SASOROV, P. V., and SCHWAGER, T., 2002, cond-mat/0208286.
[29] ALLEN, M. P., and TILDESLEY, D. J., 1987 *Computer Simulation of Liquids* (Oxford: Clarendon Press).
[30] BREY, J. J., and CUBERO, D., 1998, *Phys. Rev. E*, **57**, 2019.